Advances in Nano Research, *Vol. 4, No. 1 (2016) 51-64*
DOI: http://dx.doi.org/10.12989/anr.2016.4.1.051

On the static stability of nonlocal nanobeams using higher-order beam theories

M.A. Eltaher[*1,3], M.E. Khater[2,4], S. Park[2], E. Abdel-Rahman[2] and M. Yavuz[1]

[1]*Department of Mechanical and Mechatronics Engineering, University of Waterloo, Canada*
[2]*Department of Systems Design Engineering, University of Waterloo, Canada*
[3]*Department of Mechanical Design and Production Engineering, Zagazig University, Egypt*
[4]*Department of Mechanical Engineering, KFUPM, Dhahran 31261, KSA*

(Received January 16, 2016, Revised March 2, 2016, Accepted March 18, 2016)

Abstract. This paper investigates the effects of thermal load and shear force on the buckling of nanobeams. Higher-order shear deformation beam theories are implemented and their predictions of the critical buckling load and post-buckled configurations are compared to those of Euler-Bernoulli and Timoshenko beam theories. The nonlocal Eringen elasticity model is adopted to account a size-dependence at the nano-scale. Analytical closed form solutions for critical buckling loads and post-buckling configurations are derived for proposed beam theories. This would be helpful for those who work in the mechanical analysis of nanobeams especially experimentalists working in the field. Results show that thermal load has a more significant impact on the buckling behavior of simply-supported beams (S-S) than it has on clamped-clamped (C-C) beams. However, the nonlocal effect has more impact on C-C beams that it does on S-S beams. Moreover, it was found that the predictions obtained from Timoshenko beam theory are identical to those obtained using all higher-order shear deformation theories, suggesting that Timoshenko beam theory is sufficient to analyze buckling in nanobeams.

Keywords: buckling; nanobeams; higher-order beam theories; nonlocal elasticity; thermal loads

1. Introduction

Classical continuum mechanics approaches are commonly adopted in the analysis of nano devices because of their low computational cost, compared to molecular dynamics, and their ability to explain experimental results. Nonlocal elasticity (Eringen 1983, Peddieson *et al*. 2003) has also been adopted within this framework to account for lattice structure discontinuities, which become significant at nano-scale. Whereas continuum mechanics assumes a continuous material distribution and a point-to-point mapping between the stress and strain fields, nonlocal elasticity assumes that the stress field at a point is a function of the strain field at all points in the domain.

The classical Euler-Bernoulli beam theory (CBT) augmented with Eringen nonlocal elasticity model has been widely deployed to study the stability of nanobeams. Sudak (2003) and Adali (2008) used this approach to study the buckling of multi-walled carbon nanotubes (MWCNTs). Ghasemi *et al*. (2013) used it to study buckling and post-buckling of fluid-conveying MCNTs.

*Corresponding author, Assistant Professor, E-mail: mohaeltaher@gmail.com, mmeltaher@zu.edu.eg

 ISSN: 2287-237X (Print), 2287-2388 (Online)

Setoodeh *et al*. (2011) presented exact analytical solutions for the post-buckling configurations of single-walled carbon nanotube (SWNTs) subject to various support conditions. Ansari *et al*. (2013) studied post-buckling behavior of SWCNTs under thermal loads for various boundary conditions. Wang *et al*. (2008), Zhen and Fang (2010), Chang (2011, 2012) developed models including thermal effects to study the stability of fluid-conveying SWNTs. Murmu and Pradhan (2010) investigated the thermal stability of CNTs embedded in an elastic medium. Janghorban (2012) compared the static response of nonlocal microbeams under thermal loads obtained using two differential quadrature methods. Lim *et al*. (2012) investigated buckling of nanobeams, nanorods, and nanotubes in a temperature field. Eltaher *et al*. (2014) studied the static stability of nanowires with initial curvature under thermal loads. Besseghier *et al*. (2015) investigated nonlinear vibration of an embedded zigzag CNTs in a polymer matrix by using nonlocal CBT and energy-equivalent model.

Adali (2012) introduced nonlocal elasticity into Timoshenko beam theory (TBT) to analyze the buckling of MCNTs. Heireche *et al*. (2008) studied a wave propagation in nonlocal Timoshenko beam of single-walled CNTs. Tounsi *et al*. (2013) presented nonlocal effects on thermal buckling TBT of double-walled CNTs. Benguediab *et al*. (2014) used the same theory to investigate the effects of scale and chirality on buckling of zigzag CNTs. Narendar and Gopalakrishnan (2011), Pradhan and Mandal (2013), and Amirian *et al*. (2013) applied it to the buckling and vibrations of SWCNTs under thermal loads. Reddy and El-Borgi (2014) develop the nonlinear finite element models for nonlocal CBT and TBT that account for moderate rotations and modified von Kármán nonlinear strains.

Reddy (2007) augmented CBT, TBT, Reddy shear beam theory (RSBT), and Levinson beam theory with nonlocal elasticity to study buckling, static and dynamic behaviors of nanostructures. Emam (2013) compared static stability predictions for nanobeams obtained from CBT, TBT, and RSBT. Tounsi *et al*. (2013) studied buckling of nonlocal nanobeams under thermal loads based on a six-order shear deformation theory. A review on the state-of-the-art on nonlocal analysis for the static stability of CNTs is given in Wang *et al*. (2010). Eltaher *et al*. (2016) presented a review on nonlocal elastic models for bending, buckling, vibrations, and wave propagation of nanoscale beams.

The applicability of higher order shear theories in plate analysis is presented by many authors. Houari *et al*. (2013) developed a sin shear deformation assumption to simulate the thermoelastic bending of FG plates. Meziane *et al*. (2014) exploited previous model to study vibration and buckling of exponentially FG sandwich plate resting on elastic foundations. Tounsi *et al*. (2013) presented a refined trigonometric shear deformation theory for thermoelastic bending of FG sandwich plates. Bessaim *et al*. (2013), Belabed *et al*. (2014) and Hebali *et al*. (2014) studied bending and free vibration of FG plates with hyperbolic shear function. Zidi *et al*. (2014) presented the bending response of functionally graded material (FGM) plate resting on elastic foundation and subjected to hygro-thermo-mechanical loading using a four variable refined plate theory.

Thus far, the literature lacks a comprehensive study for the significance of implementing nonlocal elasticity models into the various available beam theories. The present work tries to fill this gap by comparing the results obtained for the static stability of nanobeams using six different beam theories adapted with Eringen nonlocal elasticity model, namely CBT, TBT, RSBT, Touratier shear beam theory (TSBT), Soldatos shear beam theory (SSBT), and Karama shear beam theory (KSBT). The beam models, developed in Section 2, account for the nonlinear von Kármán strain to allow for moderate deformations. Analytical solutions are presented in Section 3 for the

Table 1 Shear strain distribution function $\phi(z)$ for each beam theory

Theory	Abbreviation	$\phi(z)$
Euler Beam Theory	CBT	0
Timoshenko Beam Theory	TBT	z
Reddy Beam Shear Theory	RBST	$z\left(1-\frac{4z^2}{3h^2}\right)$
Touratier shear beam theory	TSBT	$\frac{h}{\pi}\sin\left(\frac{\pi z}{h}\right)$
Soldatos shear beam theory	SSBT	$h\sin h\left(\frac{\pi z}{h}\right)-z\cosh\left(\frac{1}{2}\right)$
Karama shear beam theory	KSBT	$ze^{-2\left(\frac{z}{h}\right)^2}$

buckling loads of simply-supported and clamped-clamped beams. The impact of scale effects, slenderness ratio, shear distribution, and thermal loads on the critical buckling load are investigated in Section 4. Concluding remarks are summarized in Section 5.

2. Theory and formulation

2.1 Kinematics assumptions

The axial u, and transverse w components of the beam displacement field can be described by Simsek (2010)

$$u(x,z)=u(x)-z\frac{\partial w(x)}{\partial x}+\phi(z)\,v(x) \tag{1a}$$

$$w(x,z)=w(x) \tag{1b}$$

where x is the position along the beam axis, $v(x)$ is the transverse shear strain, and $\phi(z)$ describes the shear strain distribution along the beam cross-section. The assumed shear function depends on the beam theory as listed in Table 1.

Adding von Kármán strain and thermal strain to the strain filed results in

$$\varepsilon_{xx}=\frac{\partial u}{\partial x}-z\frac{\partial^2 w}{\partial x^2}+\phi(z)\frac{\partial v}{\partial x}+\frac{1}{2}\left(\frac{\partial w}{\partial x}\right)^2-\alpha_{th}\Delta T=\varepsilon_0+zk_x+\phi(z)\frac{\partial v}{\partial x} \tag{2a}$$

$$\gamma_{xz}=\frac{\partial u}{\partial z}+\frac{\partial w}{\partial x}=-\frac{\partial w}{\partial x}+\frac{\partial \phi}{\partial z}v+\frac{\partial w}{\partial x}=\frac{\partial \phi}{\partial z}v \tag{2b}$$

where $\varepsilon_0=\frac{\partial u}{\partial x}+\frac{1}{2}\left(\frac{\partial w}{\partial x}\right)^2-\alpha_{th}\Delta T$ is the mid-plane strain and $k_x=-\frac{\partial^2 w}{\partial x^2}$ is the section strain due to bending.

2.2 Equilibrium equations

For a symmetric cross-section, the internal axial N and shear Q_s forces can be written as

$$N = \int_A E\varepsilon_{xx} dA = EA\varepsilon_0 \tag{3a}$$

$$Q_x = \int_A \frac{\partial \phi}{\partial z}(G\gamma_{xz}) dA = Gb\eta v \tag{3b}$$

where A is the cross sectional area A, b is the beam width, E is Young's modulus, G is the shear modulus, and η is defined as Emam (2013)

$$\eta = \int_{-h/2}^{h/2} \left[\frac{\partial \phi}{\partial z}\right]^2 dz$$

The resultant moment due to bending M and shear M_s can be written as

$$M = \int_A zE\varepsilon_{xx} dA = EIk_x + Eb\alpha \frac{\partial v}{\partial x} \tag{4a}$$

$$M_s = \int_A \phi(z) E\varepsilon_{xx} dA = Eb\alpha k_x + Eb\beta \frac{\partial b}{\partial x} \tag{4b}$$

where I is the second area moment and the parameters α, β are defined as Emam (2013)

$$\alpha = \int_{-h/2}^{h/2} z\phi(z) dz \quad \text{and} \quad \beta = \int_{-h/2}^{h/2} [\phi(z)]^2 dz$$

Using the principle of virtual displacement, we can write

$$0 = \int_0^L \left[\left(N\delta\varepsilon_0 + M\delta k_x + M_s \delta \frac{\partial v}{\partial x} + Q_s \delta v \right) - \left(q\delta w + \overline{P} \frac{\partial w}{\partial x} \delta \frac{\partial w}{\partial x} \right) \right] dx \tag{5}$$

where q is the transverse distributed force and $\overline{P}$ is axial compressive force applied at the boundaries. Substituting Eqs. (3) and (4) into Eq. (5), the following equilibrium equations can be obtained

$$\frac{\partial N}{\partial x} = 0 \tag{6a}$$

$$\frac{\partial}{\partial x}\left(N \frac{\partial w}{\partial x} \right) + \frac{\partial^2 M}{\partial x^2} + q - \overline{P} = 0 \tag{6b}$$

$$\frac{\partial M_s}{\partial x} - Q_s = 0 \tag{6c}$$

2.3 Nonlocal elasticity equations

The nonlocal integral constitutive equation of Eringen model can be transformed to the

following differential form (Reddy 2007, Eltaher *et al*. 2013, 2014)

$$(1-\mu\nabla^2)\sigma=\sigma_c \tag{7}$$

where ∇^2 is the Laplacian operator, σ_c and σ are the classical and nonlocal stress tensors, $\mu=e_0a$ is a scale-effect parameter, e_0 is an experimentally determined material constant, and a is a material characteristic length. For a beam, the nonlocal constitutive equation can be reduced to

$$\left(1-\mu\frac{\partial^2}{\partial x^2}\right)\sigma_{xx}=E\varepsilon_0 \tag{8a}$$

$$\left(1-\mu\frac{\partial^2}{\partial x^2}\right)\tau_{xz}=G\gamma_{xz} \tag{8b}$$

Transforming the resultants forces and moments, Eq. (3) and (4), to nonlocal domain using the differential operator of Eringen, Eq. (7), we obtain

$$\left(1-\mu\frac{\partial^2}{\partial x^2}\right)N=EA\varepsilon_0 \tag{9a}$$

$$\left(1-\mu\frac{\partial^2}{\partial x^2}\right)M=EIk_x+Eb\alpha\frac{\partial v}{\partial x} \tag{9b}$$

$$\left(1-\mu\frac{\partial^2}{\partial x^2}\right)M_s=Eb\alpha k_x+Eb\beta\frac{\partial v}{\partial x} \tag{9c}$$

$$\left(1-\mu\frac{\partial^2}{\partial x^2}\right)Q_s=Gb\eta v \tag{9d}$$

Substituting Eqs. (3) into Eq. (6), and using Eqs. (9), and performing integration by parts, the nonlocal equilibrium equations for nanobeams under thermal loads can be written as

$$\left[EI-\mu\left(\overline{P}-\frac{EA}{2L}\int_0^L\left(\frac{\partial w}{\partial x}\right)^2dx-EA\alpha_{th}\Delta T\right)\right]\frac{\partial^4 w}{\partial x^4}+\left[\overline{P}-\frac{EA}{2L}\int_0^L\left(\frac{\partial w}{\partial x}\right)^2dx-EA\alpha_{th}\Delta T\right]\frac{\partial^2 w}{\partial x^2}$$

$$-Eb\alpha\frac{\partial^3 v}{\partial x^3}+(q-\mu\, q_{,xx})=0 \tag{10a}$$

$$Eb\alpha\frac{\partial^3 w}{\partial x^3}-Eb\beta\frac{\partial^2 v}{\partial x^2}+Gb\eta v=0 \tag{10b}$$

To simplify the equations and generalize the response, the nondimensional variables $\hat{x}=x/L$, $\hat{w}=w/r$ are assumed, where $r=\sqrt{I/A}$ is the radius of gyration. Substituting into Eqs. (10) assuming no distributed transverse forces, the nondimensional equilibrium equation is obtained as (hats removed for simplicity)

$$\left[1-\bar{\mu}\left(P+N_{th}-\frac{1}{2}\int_0^1\left(\frac{\partial w}{\partial x}\right)^2 dx\right)\right]\frac{\partial^4 w}{\partial x^4}+\left(P+N_{th}-\frac{1}{2}\int_0^1\left(\frac{\partial w}{\partial x}\right)^2 dx\right)\frac{\partial^2 w}{\partial x^2}+\frac{b\alpha}{I}\frac{\partial^3 v}{\partial x^3}=0 \quad (11a)$$

$$\frac{\alpha}{I}\frac{\partial^3 w}{\partial x^3}-\frac{\beta}{I}\frac{\partial^2 w}{\partial x^2}+\frac{GL^2\eta}{EI}v=0 \quad (11b)$$

where $\bar{\mu}=\frac{\mu}{L^2}$, $P=\frac{\bar{P}L^2}{EI}$, and $N_{th}=\frac{\alpha_{th}\Delta TL^2}{r^2}$.

3. Analytical solutions

An explicit solution of critical buckling as a function of geometrical parameters, material constants, thermal load, and nonlocal scale parameter is presented in this section. The assumed displacement field in the case of simply-supported beams can be described by the following harmonic functions that satisfy the boundary conditions (Nayfeh and Emam 2008)

$$w(x)=a_1\sin\left(\frac{\pi x}{L}\right) \quad (12a)$$

$$v(x)=a_2\cos\left(\frac{\pi x}{L}\right) \quad (12b)$$

where a_1 and a_2 are, respectively, the amplitudes of maximum deflection and shear deformation of the beam that occur at midspan. Substituting Eq. (14) into the equilibrium equation, Eq. (13), yields

$$-\frac{a_2\pi^3\alpha}{\mathrm{II}}-a_1\pi^2\left(P+N_{th}-\frac{a_1{}^2\pi^2}{4}\right)+a_1\pi^4\left[1-\bar{\mu}\left(P+N_{th}-\frac{a_1{}^2\pi^2}{4}\right)\right]=0 \quad (13a)$$

$$-\frac{a_1\pi^3\alpha}{\mathrm{I}}+\frac{a_2\pi^2\beta}{\mathrm{I}}+\frac{a_2GL^2\zeta}{\mathrm{EI}}=0 \quad (13b)$$

Solving for a_1 yields a_1=0, and two stable buckling configurations

$$a_1=\mp\frac{2}{\pi}\sqrt{\frac{E\pi^4(\alpha^2-I\beta)-GIL^2\pi^2\zeta}{(EI\pi^2\beta+GIL^2\zeta)(1+\pi^2\bar{\mu})}+P+N_{th}} \quad (14)$$

The critical buckling initiates where the two stable solution branches meet at a_1=0. Thus

$$P_{cr}=\frac{E\pi^4(I\beta-\alpha^2)+GIL^2\pi^2\zeta}{(EI\pi^2\beta+GIL^2\zeta)(1+\pi^2\bar{\mu})}-N_{th} \quad (15)$$

In case of clamped-clamped boundary conditions, the displacement field can be assumed as

$$w(x)=a_1\,[1-\cos(2\pi x)] \quad (16a)$$

Table 2 Critical buckling load for different beam theories

BC	Theory	Buckling load
Simply -Supported	CBT	$\frac{\pi^2}{1+\pi^2\bar{\mu}} - N_{th}$
	TBT	$\frac{120\,G\,IL^2\pi^2 + Eh^2\pi^4(-bh^2+12\,I)}{12\,I\,(10GL^2+Eh^2\pi^2)(1+\pi^2\bar{\mu})} - N_{th}$
	RBST	$\frac{840G\,IL^2\pi^2 + E\,h^2(-7bh^2+85\,I)\pi^4}{5\,I(168\,GL^2+17\,Eh^2\pi^2)(1+\pi^2\bar{\mu})} - N_{th}$
	TSBT	$\frac{-8\,b\,Eh^5 + I\,(E\,h^2+GL^2)\pi^4}{I\,(E\,h^2+GL^2)\pi^2(1+\pi^2\bar{\mu})} - N_{th}$
	SSBT	$\frac{\pi^2(288(-2-2e+e^2)GIL^2 + Eh^2(b(35-13e)^2h^2 + 12(83+70e-37e^2)I)\pi^2)}{12\,I(24(-2-2e+e^2)GL^2 + (83+70e-37e^2)Eh^2\pi^2)(1+\pi^2\bar{\mu})} - N_{th}$
	KSBT	$\frac{4GIL^2\pi^2(-2+3e\sqrt{\pi}Erf[1]) - Eh^2\pi^4(-2I(-2+e\sqrt{\pi}Erf[1]) + bh^2(2-2\sqrt{2e\pi}Erf[\frac{1}{\sqrt{2}}] + e\pi Erf[\frac{1}{\sqrt{2}}]^2))}{2I(1+\pi^2\bar{\mu})(Eh^2\pi^2(-2+e\sqrt{\pi}Erf[1]) + 2GL^2(-2+3e\sqrt{\pi}Erf[1]))} - N_{th}$
Clamped-Clamped	CBT	$\frac{4\pi^2}{1+4\pi^2\bar{\mu}} - N_{th}$
	TBT	$\frac{60G\,IL^2\pi^2 - 2\,Eh^2(bh^2-12\,I)\pi^4}{3\,I(5GL^2+2\,Eh^2\pi^2)(1+4\pi^2\bar{\mu})} - N_{th}$
	RBST	$\frac{840\,G\,I\,L^2\pi^2 + 4\,E\,h^2(-7bh^2+85\,I)\pi^4}{5\,I\,(42\,GL^2+17\,Eh^2\pi^2)(1+4\pi^2\bar{\mu})} - N_{th}$
	TSBT	$\frac{-128\,b\,Eh^5 + 4\,I\,(4\,Eh^2+GL^2)\pi^4}{I\,\pi^2(4\,Eh^2+GL^2)(1+4\pi^2\bar{\mu})} - N_{th}$
	SSBT	$\frac{\pi^2(72(-2-2e+e^2)GIL^2 + E\,h^2(b(35-13e)^2h^2 + 12(83+70e-37e^2)I)\pi^2)}{3\,I(6(-2-2e+e^2)GL^2 + (83+70e-37e^2)Eh^2\pi^2)(1+4\pi^2\bar{\mu})} - N_{th}$
	KSBT	$\frac{4(GIL^2\pi^2(3e\sqrt{\pi}Erf[1]-2) - E\,h^2\pi^4(2\,I(2-e\sqrt{\pi}Erf[1]) - bh^2(2-2\sqrt{2e\pi}Erf[\frac{1}{\sqrt{2}}] + e\pi\,Erf[\frac{1}{\sqrt{2}}]^2)))}{I\,(1+4\pi^2\bar{\mu})(2\,Eh^2\pi^2(-2+e\sqrt{\pi}Erf[1]) + GL^2(-2+3e\sqrt{\pi}Erf[1]))} - N_{th}$

$$v(x)=a_2 \sin(2\pi x) \tag{16b}$$

Substituting Eq. (16) into the equilibrium equation and solving for a_1 results in a_1=0 and two stable solutions described by

$$a_1 = \mp\frac{2}{\pi}\sqrt{\frac{16E\pi^4(\alpha^2 - I\beta) - 4GIL^2\pi^2\zeta}{(4EI\pi^2\beta + GIL^2\zeta)(1+4\pi^2\bar{\mu})} + P + N_{th}} \tag{17}$$

The critical buckling is then derived as

$$P_{cr} = \frac{16E\pi^4(I\beta - \alpha^2) + 4GIL^2\pi^2\zeta}{(4EI\pi^2\beta + GIL^2\zeta)(1+4\pi^2\bar{\mu})} - N_{th} \tag{18}$$

Table 2 summarizes the critical buckling loads for simply-supported and clamped-clamped nanobeams implementing different beam theories.
where the error function *Erf (n)* is defined as

$$Erf(n) = \frac{2}{\sqrt{\pi}}\int_0^n e^{-\tau^2} d\tau$$

Table 3 Critical buckling load for S-S nanobeam with different *L/h* and $\bar{\mu}$ at N_{th}=0

L/h	$\bar{\mu}$	CBT	TBT	RBST	TSBT	SSBT	KSBT
100	**0**	9.8696	9.86707	9.86707	9.86708	9.86707	9.86709
	0.01	8.98302	8.98071	8.98071	8.98072	8.98071	8.98073
	0.02	8.24258	8.24047	8.24047	8.24047	8.24047	8.24048
	0.03	7.61492	7.61296	7.61296	7.61297	7.61296	7.61298
	0.04	7.07608	7.07426	7.07426	7.07427	7.07426	7.07428
	0.05	6.60846	6.60676	6.60676	6.60677	6.60676	6.60677
10	**0**	9.8696	9.62268	9.62275	9.62312	9.62275	9.62422
	0.01	8.98302	8.75827	8.75834	8.75867	8.75834	8.75968
	0.02	8.24258	8.03636	8.03642	8.03673	8.03643	8.03765
	0.03	7.61492	7.4244	7.42446	7.42474	7.42446	7.42559
	0.04	7.07608	6.89904	6.8991	6.89936	6.8991	6.90015
	0.05	6.60846	6.44312	6.44317	6.44342	6.44317	6.44416

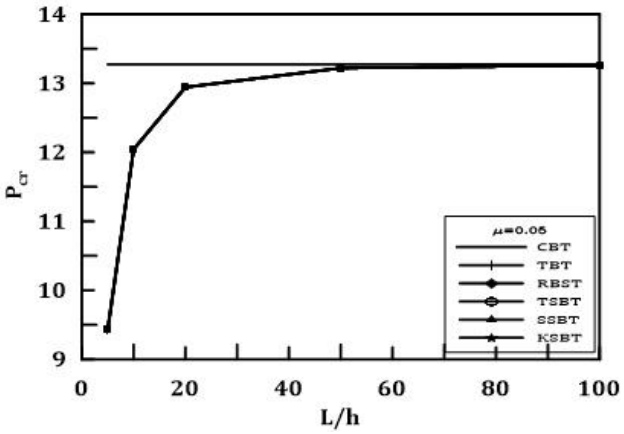

Fig. 1 Effect of slenderness ratio on a critical buckling load for C-C beam at μ=0.05

4. Results

Numerical results presented in this section show the effects of shear deformation functions, nonlocal parameter, thermal load, slenderness ratio, and boundary conditions on the critical buckling loads and their amplitudes. The material and geometry parameters assumed throughout the analysis are E=30 GPa, v=0.3, h=1 nm, b=1 nm, a=23.1×10^{-6} 1/K for slenderness ratio L/h=10 and 100.

4.1 Zero thermal load analysis

Table 3 illustrates the variation of critical buckling with respect to nonlocal scale parameter, proposed theories, and slenderness ratios. For all theories, it is noted that the buckling load decreases as the nonlocal parameter increases at a specified slenderness ratio. Moreover, for high

slenderness (L/h=100) ratio, all theories are approximately identical in predicting the buckling load, which confirms the accuracy of the simple Euler-Bernoulli theory in the case of thin nanobeams. However, the discrepancy between Euler theory and other theories is noticeable for a moderately thick beam (L/h=10). On the other hand, the results obtained using the Timoshenko beam theory (TBT) coincide with those obtained using higher-order theories suggesting the accuracy of using TBT for the case of moderately thick beams. Our results are in good agreement with those obtained by Emam (2013) for Euler, Timoshenko, and Reddy beam theories.

Fig. 1 illustrates the effect of slenderness ratio on the buckling of clamped-clamped beam at μ=0.05. As depicted in the figure, all theories are identical in the region $50 \leq L/h \leq 100$. However, critical buckling of CBT is overestimated in the region $L/h \leq 50$. The deviation between CBT and shear deformation theories increases as L/h decreases. This deviation increases smoothly from 0 % to 9.3% as L/h decreases from 50 to 10. However, this deviation increased exponentially for moderated thick beams ($5 < L/h < 10$).

The effects of nonlocal parameter on the post-buckling amplitude for S-S and C-C moderately thick nanobeams (L/h=10) are presented in Figs. 2 and 3, respectively. It is noted that as the nonlocal parameter increases, the critical buckling decreases and amplitude of post-buckling increases for both S-S and C-C nanobeam. However, the effect of nonlocal parameter is more significant in case of C-C nanobeam than that in S-S beams as illustrated in Figs. 2 and 3.

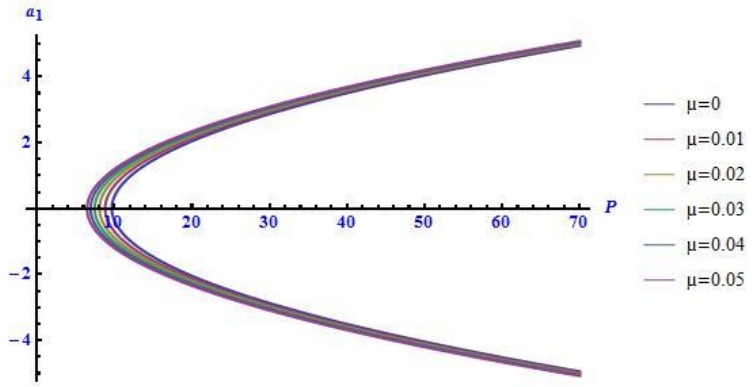

Fig. 2 Effect of nonlocal parameter on a postbuckling amplitude for S-S TBT at L/h=10

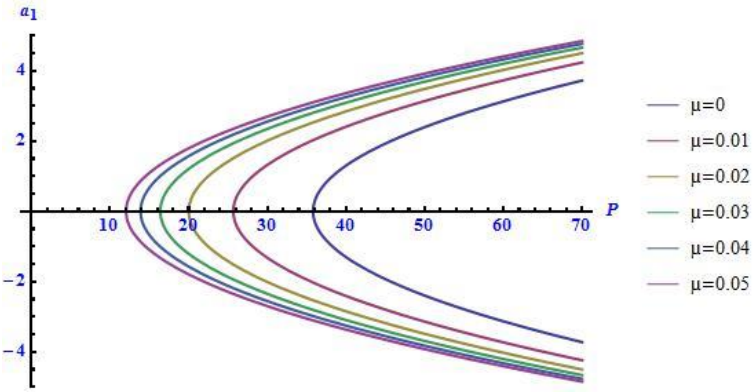

Fig. 3 Effect of nonlocal parameter on a postbuckling amplitude for C-C TBT at L/h=10

Table 4 Critical buckling load for a S-S nanobeam with L/h=10

ΔT	μ	CBT	TBT	RBST	TSBT	SSBT	KSBT
0	**0**	9.8696	9.62268	9.62275	9.62312	9.62275	9.62422
	0.01	8.98302	8.75827	8.75834	8.75867	8.75834	8.75968
	0.02	8.24258	8.03636	8.03642	8.03673	8.03643	8.03765
	0.03	7.61492	7.4244	7.42446	7.42474	7.42446	7.42559
25	**0**	9.1766	8.92968	8.92975	8.93012	8.92975	8.93122
	0.01	8.29002	8.06527	8.06534	8.06567	8.06534	8.06668
	0.02	7.54958	7.34336	7.34342	7.34373	7.34343	7.34465
	0.03	6.92192	6.7314	6.73146	6.73174	6.73146	6.73259
50	**0**	8.4836	8.23668	8.23675	8.23712	8.23675	8.23822
	0.01	7.59702	7.37227	7.37234	7.37267	7.37234	7.37368
	0.02	6.85658	6.65036	6.65042	6.65073	6.65043	6.65165
	0.03	6.22892	6.0384	6.03846	6.03874	6.03846	6.03959

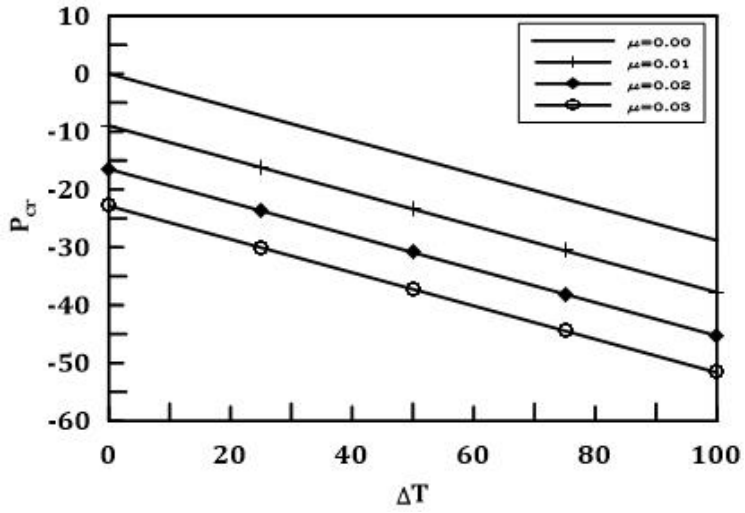

Fig. 4 Effect of temperature on a critical buckling at different μ for S-S TBT at L/h=10

4.2 Thermal load effect

This section is devoted to studying the effect of thermal load on the critical buckling load and post-buckling amplitudes for both S-S and C-C nanobeams under different beam theories. Table 4 illustrates the variation of buckling loads with temperature, which indicates a decrease in buckling load with increase in temperature difference ΔT. The percentage change in critical buckling load with respect to thermal load is presented in Fig. 4, which shows a linear decrease in buckling load with respect to temperature difference. The critical buckling decreases to 29 % when ΔT increases by a 100. However, the buckling load decreases to 25% as the nonlocal parameter increases from 0 to 0.03. Fig. 5 illustrates the effect of temperature difference on post-buckling amplitudes, which indicates a small temperature effect on the amplitude in the case of S-S nanobeams.

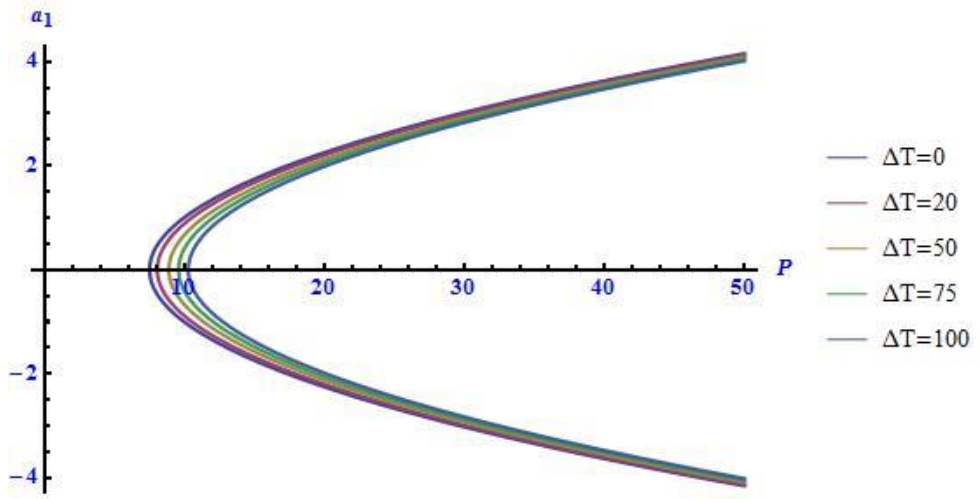

Fig. 5 Effect of ΔT on a post-buckling amplitude for S-S TBT at L/h=10 and μ=0.03

Table 5 Critical buckling load for a C-C nanobeam with L/h=10

ΔT	μ	**CBT**	**TBT**	**RBST**	**TSBT**	**SSBT**	**KSBT**
0	**0**	39.4784	35.8034	35.8075	35.8132	35.8074	35.8293
	0.01	28.3043	25.6695	25.6724	25.6765	25.6724	25.6881
	0.02	22.0603	20.0067	20.009	20.0122	20.009	20.0212
	0.03	18.0733	16.3909	16.3927	16.3954	16.3927	16.4027
20	**0**	38.7854	35.1104	35.1145	35.1202	35.1144	35.1363
	0.01	27.6113	24.9765	24.9794	24.9835	24.9794	24.9951
	0.02	21.3673	19.3137	19.316	19.3192	19.316	19.3282
	0.03	17.3803	15.6979	15.6997	15.7024	15.6997	15.7097
50	**0**	38.0924	34.4174	34.4215	34.4272	34.4214	34.4433
	0.01	26.9183	24.2835	24.2864	24.2905	24.2864	24.3021
	0.02	20.6743	18.6207	18.623	18.6262	18.623	18.6352
	0.03	16.6873	15.0049	15.0067	15.0094	15.0067	15.0167

The effect of temperature on the critical buckling load for C-C nanobeam is presented in Table 5. The table shows a decrease in the buckling load with increase in temperature which highlights the significance of temperature on the buckling loads. The qualitative representation of Table 5 describing the percentage change in critical buckling load with respect to temperature change and length-scale effect is presented in Fig. 6. It is noticed that, by fixing the temperature and varying the nonlocal parameter from 0 to 0.01, 29% reduction in critical buckling load is observed. However, increasing the nonlocal parameter from 0.02 to 0.03 results in 10% decrease in critical buckling load. So, it can be concluded that the buckling load is highly increased with higher values of the nonlocal parameter. For the case in hand, changing the temperature by 100 causes a decrease in buckling load by 19%. Fig. 7 shows the effect of temperature difference on the amplitude of post-buckling for C-C nanobeams.

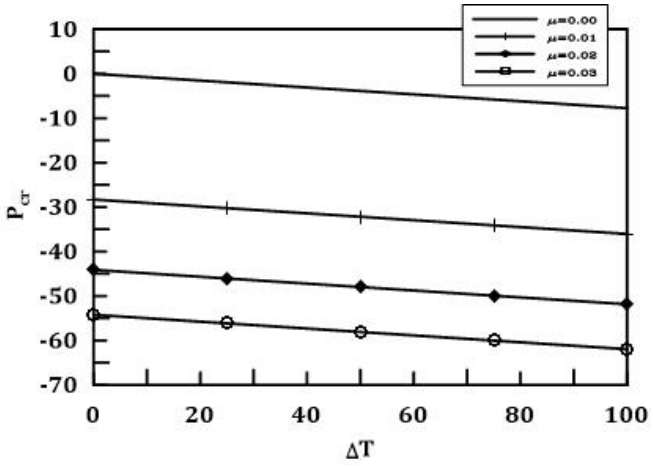

Fig. 6 Effect of temperature on a critical buckling at different μ for C-C TBT at L/h=10

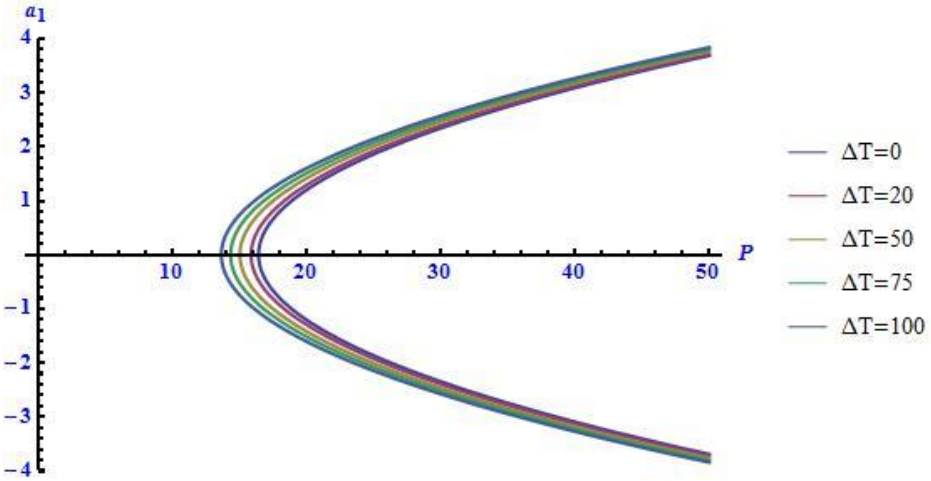

Fig. 7 Effect of ΔT on a post-buckling amplitude for C-C TBT at L/h=10 and μ=0.03

5. Conclusions

The buckling loads and post-buckling amplitudes of nonlocal nanobeams under mechanical and thermal loads are analytically obtained using higher-order beam theories and compared against Euler and Timoshenko theories results. The nonlocal Eringen's elasticity model is adopted to account for small-scale effects. The critical buckling loads and post-buckling amplitudes of a nanobeam with varying nonlocal parameter, slenderness ratio, shear distribution, thermal loads for simply-supported and clamped-clamped nanobeams are presented. The results show that the nonlocal parameter has a notable effect on the buckling loads and post-buckling amplitudes where the nonlocal effect is more significant for clamped-clamped beams than for simply-supported beams. It was observed that the thermal load tends to decrease the critical buckling load, thus reflecting the effect of environment temperature on the behavior of nanobeams. Comparing the results obtained by the different beam theories, it was found that the classical Euler beam theory is

accurate for high slenderness ratios ($50 \leq L/h \leq 100$), whereas Timoshenko beam theory is more accurate for moderately thick beams ($L/h \leq 50$) with negligible improvement by higher-order theories.

References

Adali, S. (2008), "Variational principles for multi-walled carbon nanotubes undergoing buckling based on nonlocal elasticity theory", *Phys. Lett. A*, **372**(35), 5701-5705.

Adali, S. (2012), "Variational formulation for buckling of multi-walled carbon nanotubes modelled as nonlocal Timoshenko beams", *J. Theo. Appl. Mech.*, **50** (1), 321-333.

Ansari, R., Gholami, R. and Sahmani, S. (2013), "Prediction of compressive post-buckling behavior of single-walled carbon nanotubes in thermal environments", *Appl. Phys. A*, **113**(1), 145-153.

Amirian, B., Hosseini-Ara, R. and Moosavi, H. (2013), "Thermo-mechanical vibration of short carbon nanotubes embedded in pasternak foundation based on nonlocal elasticity theory", *Shock Vib.*, **20**(4), 821-832.

Belabed, Z., Houari, M.S.A., Tounsi, A., Mahmoud, S.R. and Bég, O.A. (2014), "An efficient and simple higher order shear and normal deformation theory for functionally graded material (FGM) plates", *Compos. Part B: Eng.*, **60**, 274-283.

Benguediab, S., Tounsi, A., Zidour, M. and Semmah, A. (2014), "Chirality and scale effects on mechanical buckling properties of zigzag double-walled carbon nanotubes", *Compos. Part B: Eng.*, **57**, 21-24.

Benzair, A., Besseghier, A., Heireche, H., Bousahla, A.A. and Tounsi, A. (2015), "Nonlinear vibration properties of a zigzag single-walled carbon nanotube embedded in a polymer matrix", *Adv. Nano Res.*, **3**(1), 029.

Bessaim, A., Houari, M.S., Tounsi, A. and Mahmoud, S.R., (2013), "A new higher-order shear and normal deformation theory for the static and free vibration analysis of sandwich plates with functionally graded isotropic face sheets", *J. Sandw. Struct. Mater.*, **15**(6), 671-703.

Chang, T. (2011), "Thermal-nonlocal vibration and instability of single-walled carbon nanotubes conveying fluid", *J. Mech.*, **27** (04), 567-573.

Chang, T. (2012), "Thermal-mechanical vibration and instability of a fluid-conveying single-walled carbon nanotube embedded in an elastic medium based on nonlocal elasticity theory", *Appl. Math. Model.*, **36**(5), 1964-1973.

Eltaher, M., Khater, M., Abdel-Rahman, E. and Yavuz, M. (2014), "A Model for Nano Bonding Wires under Thermal Loading", *IEEE-Nano 2014, Toronto*, Canada.

Eltaher, M., Emam, S. and Mahmoud, F. (2013), "Static and stability analysis of nonlocal functionally graded nanobeams", *Compos. Struct.*, **96**, 82-88.

Eltaher, M., Khairy, A., Sadoun, A. and Omar, F. (2014), "Static and buckling analysis of functionally graded Timoshenko nanobeams", *Appl. Math. Comput.*, **229**, 283-295.

Eltaher, M.A., Khater, M.E. and Emam, S.A. (2016), "A review on nonlocal elastic models for bending, buckling, vibrations, and wave propagation of nanoscale beams", *Appl. Math. Model.*, **40**(5-6), 4109-4128.

Emam, S. (2013), "A general nonlocal nonlinear model for buckling of nanobeams", *Appl. Math. Model.*, **37**(10), 6929-6939.

Eringen, A. (1983), "On differential equations of nonlocal elasticity and solutions of screw dislocation and surface waves", *J. Appl. Phys.*, **54**(9), 4703-4710.

Ghasemi, A., Dardel, M., Ghasemi, M. and Barzegari, M. (2013), "Analytical analysis of buckling and post-buckling of fluid conveying multi-walled carbon nanotubes", *Appl. Math. Model.*, **37**(7), 4972-4992.

Hebali, H., Tounsi, A., Houari, M.S.A., Bessaim, A. and Bedia, E.A.A. (2014), "New quasi-3D hyperbolic shear deformation theory for the static and free vibration analysis of functionally graded plates", *J. Eng. Mech.*, **140**(2), 374-383.

Heireche, H., Tounsi, A., Benzair, A., Maachou, M. and Bedia, E.A. (2008), "Sound wave propagation in single-walled carbon nanotubes using nonlocal elasticity", *Physica E*, **40**(8), 2791-2799.
Houari, M.S.A., Tounsi, A. and Bég, O.A. (2013), "Thermoelastic bending analysis of functionally graded sandwich plates using a new higher order shear and normal deformation theory", *Int. J. Mech. Sci.*, **76**, 102-111.
Janghorban, M. (2012), "Two different types of differential quadrature methods for static analysis of microbeams based on nonlocal thermal elasticity theory in thermal environment", *Arch. Appl. Mech.*, **82**(5), 669-675.
Lim, C., Yang, Q. and Zhang, J. (2012), "Thermal buckling of nanorod based on non-local elasticity theory", *Int. J. Nonlin. Mech.*, **47**(5), 496-505.
Narendar, S. and Gopalakrishnan, S. (2011), "Critical buckling temperature of single-walled carbon nanotubes embedded in a one-parameter elastic medium based on nonlocal continuum mechanics", *Physica E*, **43**(6), 1185-1191.
Nayfeh, A. and Emam, S. (2008), "Exact solution and stability of postbuckling configurations of beams", *Nonlin. Dyn.*, **54**(4), 395-408.
Meziane, M.A.A., Abdelaziz, H.H. and Tounsi, A. (2014), "An efficient and simple refined theory for buckling and free vibration of exponentially graded sandwich plates under various boundary conditions", *J. Sandw. Struct. Mater.*, **16**(3), 293-318.
Murmu, T. and Pradhan, S. (2010), "Thermal effects on the stability of embedded carbon nanotubes", *Comput. Mater. Sci.*, **47**(3), 721-726.
Peddieson, J., Buchanan, G. and McNitt, R.P. (2003), "Application of nonlocal continuum models to nanotechnology", *Int. J. Eng. Sci.*, **41**, 305-312.
Pradhan, S. and Mandal, U. (2013), "Finite element analysis of CNTs based on nonlocal elasticity and Timoshenko beam theory including thermal effect", *Physica E*, **53**, 223-232.
Reddy, J. (2007), "Nonlocal theories for bending, buckling and vibration of beams", *Int. J. Eng. Sci.*, **45**(2), 288-307.
Reddy, J.N. and El-Borgi, S. (2014), "Eringen's nonlocal theories of beams accounting for moderate rotations", *Int. J. Eng. Sci.*, **82**, 159-177.
Setoodeh, A., Khosrownejad, M. and Malekzadeh, P. (2011), "Exact nonlocal solution for postbuckling of single-walled carbon nanotubes", *Physica E*, **43**(9), 1730-1737.
Şimşek, M. (2010), "Fundamental frequency analysis of functionally graded beams by using different higher-order beam theories", *Nucl. Eng. Des.*, **240**(4), 697-705.
Sudak, L. (2003), "Column buckling of multiwalled carbon nanotubes using nonlocal continuum mechanics", *J. Appl. Phys.*, **94**(11), 7281-7287.
Tounsi, A., Semmah, A. and Bousahla, A. (2013), "Thermal buckling behavior of nanobeams using an efficient higher-order nonlocal beam theory", *J. Nanomech. Micromech.*, **3**(3), 37-42.
Tounsi, A., Houari, M.S.A. and Benyoucef, S. (2013), "A refined trigonometric shear deformation theory for thermoelastic bending of functionally graded sandwich plates", *Aerosp. Sci. Tech.*, **24**(1), 209-220.
Tounsi, A., Benguediab, S., Adda, B., Semmah, A. and Zidour, M. (2013), "Nonlocal effects on thermal buckling properties of double-walled carbon nanotubes", *Adv. Nano Res.*, **1**(1), 1-11.
Wang, C., Zhang, Y., Xiang, Y. and Reddy, J. (2010), "Recent studies on buckling of carbon nanotubes", *Appl. Mech. Rev.*, **63**(3), 030804.
Wang, L., Ni, Q., Li, M. and Qian, Q. (2008), "The thermal effect on vibration and instability of carbon nanotubes conveying fluid", *Physica E*, **40**(10), 3179-3182.
Zhen, Y. and Fang, B. (2010), "Thermal-mechanical and nonlocal elastic vibration of single-walled carbon nanotubes conveying fluid", *Comput. Mater. Sci.*, **49**(2), 276-282.
Zidi, M., Tounsi, A., Houari, M.S.A. and Bég, O.A. (2014), "Bending analysis of FGM plates under hygro-thermo-mechanical loading using a four variable refined plate theory", *Aerosp. Sci. Tech.*, **34**, 24-34.